Pharmacogn. Mag.
A multifaceted peer reviewed journal in the field of Pharmacognosy and Natural Products
www.phcog.com | www.phcog.net

ORIGINAL ARTICLE

Aroma Characteristic Analysis of *Amomi fructus* from Different Habitats using Machine Olfactory and Gas Chromatography-Mass Spectrometry

Huaying Zhou[1,2], Dehan Luo[1], Hamid Gholamhosseini[3], Zhong Li[4], Bin Han[4], Jiafeng He[1], Shumei Wang[4]

[1]Department of Communication, School of Information Engineering, Guangdong University of Technology, [2]Department of Computer Science, College of Medical Information Engineering, Guangdong Pharmaceutical University, [4]Department of Traditional Chinese Medicine Resources, College of Traditional Chinese Medicine, Guangdong Pharmaceutical University, Guangzhou, China, [3]Department of Electrical and Electronic Engineering, School of Engineering, Computer and Mathematical Sciences, Auckland University of Technology, Auckland, New Zealand

Submitted: 30-12-2018 Revised: 12-02-2019 Published: 16-05-2019

ABSTRACT

Background: *Amomi fructus* (*AF* Lour.) has been used to treat digestive diseases in the context of Traditional Chinese Medicine. Its aroma characteristics have been attracted attention and are considered to be effective markers for determining *AF* from different habitats. **Materials and Methods:** In this article, the odor characteristics of *AF* from three different habitats were investigated and analyzed using gas chromatography-mass spectrometry (GC-MS) and an electronic nose (E-nose). **Results:** It was found that the E-nose in conjunction with principal component analysis as an analytic tool, showed good performance and achieved a total variance of 93.90% with the first two principal components. A total of 65 aroma constituents among three groups of *AF* were separated, identified, and calculated using GC-MS. It was observed that the components and the contents were clearly different among the three groups. To confirm the interrelation between aroma constituents and sensors, the contents of 12 aroma ingredients and the response values of six sensors were selected to be trained and tested using the partial least squares. A satisfied quantitative prediction was presented that the contents of selected constituents were accurately predicted by corresponding E-nose sensors with the most determination coefficient of calibration and determination coefficient of prediction of >90%. **Conclusion:** It was revealed that the E-nose is capable of discriminating *AF* from different habitats, presenting an accurate, easy-operating, and nondestructive reference approach.

Key words: *Amomi fructus*, aroma analysis, electronic nose, gas chromatography-mass spectrometry, machine olfactory

SUMMARY

In this article, odor characteristics of *Amomi fructus* (*AF*) from three different habitats were investigated and analyzed using gas chromatography-mass spectrometry (GC-MS) and an electronic nose (E-nose). From the experimental results, the following conclusions were drawn:

- The components and the contents of *AF* were clearly different among Guangdong Sharen, Guangxi Sharen, and Hainan Sharen; the analysis results confirmed by E-nose were similar to that of GC-MS
- The six sensors (S1, S3, S5, S7, S8, and S9 in PEN3) were highly related to three main volatile components (terpenes, alcohols, and esters) of *AF*, which enabled the E-nose to differentiate the three groups of *AF* successfully
- A satisfied quantitative prediction was showed that the contents of selected constituents were accurately predicted by six E-nose sensors with most $(R_c)^2$ and $(R_p)^2$ >90%.

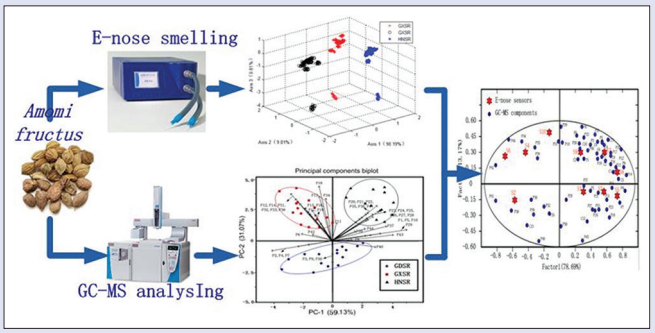

Abbreviations used: TCM: Traditional Chinese medicine; GC-MS: Gas chromatography-mass spectrometry; E-nose: Electronic nose; PCA: Principal component analysis; PLS: Partial least squares; $(R_c)^2$: Determination coefficient of calibration; $(R_p)^2$: Determination coefficient of prediction; *AF*: *Amomi fructus*; TLC: Thin-layer chromatography; HPLC: High-performance liquid chromatography; CE-DAD: Capillary electrophoresis diode array detection; DFA: Discriminant factorial analysis; GDSR: Guangdong Sharen; GXSR: Guangxi Sharen; HNSR: Hainan Sharen; MOS: Metal oxide semiconductor; RSD: Relative standard deviation; BOOAS: Bionic olfactory odor analysis software; NIST: National institute of standards and technology; RC: Relative content; SD: Standard deviation; RMSEC: Root mean square of calibration; RMSEP: Root mean square error of prediction.

Correspondence:

Prof. Dehan Luo,
Department of Communication, School of Information Engineering, Guangdong University of Technology, Guangzhou 510006, China.
E-mail: dehanluo@gdut.edu.cn

DOI: 10.4103/pm.pm_665_18

Access this article online
Website: www.phcog.com
Quick Response Code:

INTRODUCTION

Amomi fructus (*AF*) is the dried and mature fruit of *AF* Lour., *AF* Lour. var. *xanthioides* T. L. Wu et Senjen, or *Amomum longiligulare* T. L. Wu. As an essential Traditional Chinese Medicine with various activities (such as eliminating damp, improving appetite, warming the spleen, checking diarrhea, and preventing abortion) and anti-inflammatory and analgesic effects, it has been reported and widely used as an excellent crude drug for the treatment of digestive system and respiratory system diseases.[1,2] One of the main components of volatile oil in *AF*, bornyl

This is an open access journal, and articles are distributed under the terms of the Creative Commons Attribution-NonCommercial-ShareAlike 4.0 License, which allows others to remix, tweak, and build upon the work non-commercially, as long as appropriate credit is given and the new creations are licensed under the identical terms.

For reprints contact: reprints@medknow.com

Cite this article as: Zhou H, Luo D, Gholamhosseini H, Li Z, Han B, He J, *et al*. Aroma characteristic analysis of *Amomi fructus* from different habitats using machine olfactory and gas chromatography-mass spectrometry. Phcog Mag 2019;15:392-401.

© 2019 Pharmacognosy Magazine | Published by Wolters Kluwer - Medknow

acetate, has a significant effect on anti-inflammatory and analgesic to animals;[3] volatile oil of *AF* also has significant therapeutic functions in antioxidation, antibiosis, and hypoglycemic.[1,4] Besides, *AF* is authorized as a food by the China Food and Drug Administration and can be used to make delicious dishes and soup.[5] There are several growing areas for *AF*, such as Guangdong, Guangxi, and Hainan provinces of China. However, *AF* from different habitats has similar appearance, but with different quality and therapeutic effect. Guangdong *AF* has the best quality and efficacy for treatment,[6] but it is very difficult to distinguish *AF* from other habitats using traditional sensory methods.

Human sensory evaluation[7] and chemical composition analysis[8] are two conventional methods for distinguishing *AF* from different growing regions. The human vision, taste, and smell approach is subjective with low accuracy and limited functionality.[9] While the chemical composition analysis such as thin-layer chromatography (TLC), high-performance liquid chromatography (HPLC) and capillary electrophoresis (CE),[10,11] identify *AF* based on chemical composition indexes. They are intuitive and effective detection methods, but suffer from being a complex operation, time-consuming, costly and destructive, and cannot meet the need for real-time and nondestructive detection. Therefore, new applicable and nondestructive analysis methods based on efficient features and aroma characteristics are attracting more attention.

Electronic nose (E-nose) is an instrument for detecting and identifying of volatile compounds by mimicking the olfactory system of animals.[12] It has been widely used in medicines,[13,14] food industry,[15,16] and environmental monitoring.[17,18] E-nose can combine the advantage of sensory evaluation and GC-MS, providing outputs similar to GC-MS nondestructively.[19] Zhou X presented a novel approach using an E-nose based on metal oxide sensors to identify whether *Pinelliae rhizoma* was fumed with sulfur and to predict the fuming degree of *P. rhizoma*. Multivariate statistical methods such as principal components analysis (PCA), discriminant factorial analysis, and partial least squares (PLS) were used for data analyzing and identification.[20] Li *et al*. put forward a new headspace integrated E-nose to distinguish six groups of Chinese medical herbs and found its performance of correct classification rate for discriminating 13 species of herbs was 100%, which showed the potential application of the E-nose for on-site volatiles analysis.[21] However, few researches have focused explicitly on the aroma characteristics of *AF* with the E-nose technology.

In this article, an E-nose was used to investigate the aroma fingerprint characteristics of *AF* from different growing regions, and GC-MS equipment was employed to analyze the volatile components of *AF* samples. Then, PCA was used to build a model for comparing E-nose and GC-MS data. Finally, a fast and nondestructive prediction model was built to identify different *AF* growing regions. The purposed study could provide reference for a real-time, easy, accurate, and nondestructive method for identifying different regions of growing *AF*.

MATERIALS AND METHODS

Amomi fructus materials

AF samples were collected from three original growing locations, Yangchun City of Guangdong, Ningming County of Guangxi, Chengmai County of Hainan, in China, labeled as Guangdong Sharen (GDSR), Guangxi Sharen (GXSR), and Hainan Sharen (HNSR), respectively. All samples were harvested in July 2017 and dried at low temperature. They were collected by the fourth author (Zhong Li) and were verified by the fifth author (Bin Han). During E-nose analysis and GC-MS detection, experimental conditions were optimized, and *AF* samples were tested under the optimized condition. For further data collection and analysis by E-nose and GC-MS, the *AF* samples were grouped in two different sealed bags and stored in a vacuum dryer.

Preparation of volatile oil

For extraction of *AF* volatile oil, we followed the method developed in General Principle 2204 of the fourth edition in Chinese Pharmacopoeia (2015 edition).[2] Accordingly, *AF* samples were first sliced into pieces and then milled into powder and sieved with 24 meshes so, a total of 45 samples (15 GDSR, 15 GXSR and 15 HNSR) and each sample weighed 50 g was extracted. We used a Soxhlet extractor (SER148/6; VELP, Usmate Velate, Italy) in ethyl ether for 5 h and evaporated (110–120°C) the samples after collection. The ethyl ether was extracted with 500 mL of water with a steam distillation for 10 h, and the yield rate was calculated using the following equation:

$$W(\%) = \frac{m_1}{m_2} \times 100 \quad (1)$$

Where W is the yield rate, m_1 is the volatile oil weight, and m_2 denotes *AF* weight. The same recovered volatile oil was diluted and used for further GC-MS determination.

Electronic nose

The PEN3 E-nose (Airsense Analytics, Schwerin, Germany) was used in this study. It consists of an automatic sampling device, an array of sensors, and a computer signal preprocessing system. It has a compact measurement room, that is, an array of 10 metal oxide semiconductor (MOS) sensors for different sensing materials. Table 1 shows the list of sensors and their characteristics. A thermostat (JB-3A, Leici Ltd., Shanghai, China) was used to heat samples.

Before data collection, the E-nose system was connected to a computer and run for at least 60 min to ensure all the sensors were heated up to the working temperature (above 200°C) and the gas path was cleaned by clean air. The parameters of PEN3 were optimized for the best working condition. The total of 45 samples (15 GDSR, 15 GXSR, and 15 HNSR) were put into a glass beaker (500 mL) and sealed with plastic wrap. The beaker was kept for 30 min (headspace-generated time) at the room

Table 1: The name and characteristics of each sensor in PEN3

Sensor number	Sensor name	Object substances for sensing	Threshold value (mL/m^3)
S1	W1C	Aromatics	10
S2	W5S	Nitrogen oxides	1
S3	W3C	Ammonia and aromatic molecules	10
S4	W6S	Hydrogen	100
S5	W5C	Methane, propane, and aliphatic nonpolar molecules	1
S6	W1S	Broad methane	100
S7	W1W	Sulfur-containing organics	1
S8	W2S	Broad alcohols	100
S9	W2W	Aromatics, sulfur- and chlorine-containing organics	1
S10	W3S	Methane and aliphatics	10

PEN3: An E-nose (Airsense Analytics, Schwerin, Germany)

temperature to ensure that enough smell was emitted from samples and get equilibrium. To obtain a steady-state data collection, each sample was continuously detected 12 times and each time included monitoring process (120 s) and cleaning process (180 s). The chamber flow was set at 150 mL/min and the injection flow was set at 150 mL/min.

On the completion of data detection, there were 12 data files and each file contained 120 × 10 samples (120 s for the measurement of 10 sensors). The data matrix (120 × 10) was automatically recorded by the Bionic Olfactory Odor Analysis Software (BOOAS version 2.0, Guangdong University of Technology, Guangzhou, China) as the raw data for the following analysis. Hence, overall, there were 540 (45 × 12 = 540) data files.

Gas chromatography-mass spectrometry

Before data collection, volatile oil of GDSR, GXSR, and HNSR were diluted 100 times with ethyl ether separately to obtain an effective GC-MS spectrogram. These volatile oil compounds were identified using a GC system (Agilent 7890A, USA) equipped with HP-5 capillary column and MS system (Agilent 5975C, USA). After optimizing the selected GC and MSD parameters, the following conditions were set:

1. GC conditions: HP-5 Methyl Siloxane chromatographic column with an ID of 320 μm and film thickness of 0.25 μm. The temperature of the injection port was kept at 250°C, the interface temperature was set at 230°C, and high-purity helium was used as the carrier gas. The oven temperature was set according to the following steps: initial temperature 60°C, kept for 3 min, ramped to 130°C at 20°C/min and then ramped to 160°C at 5°C/min, held for 10 min, and finally ramped to 230°C at 20°C/min and kept for 2 min. Then, the system was reset for 15 min. The flow program was set as follow: the rate was 1.00 mL/min; injection volume was 1 μL, and the gasification chamber temperature was kept on 280°C
2. MS conditions: The ionization mode was electron bombardment ionization source, with electron energy of 70 eV, the ionization temperature was held at 230°C, the interface temperature was set at 280°C with temperature quadrupole at 150°C, solvent was delayed for 3 min and the acceleration voltage was set 34.6 V, the multiplier voltage was maintained at 1388 V, quantity scanning range was from 40 amu to 500 amu, and the quantity scanning speed was set 2.94 times/s.

To get the average values of the relative standard deviation (RSD) of *AF* volatile oil, ten replicated samples were selected from each group of *AF* volatile oil and each sample was measured in three times by GC-MS within the same condition. Finally, the average value was computed from 90 detection times (total, 10 × 3 × 3 = 90).

Repeatability of electronic nose and gas chromatography-mass spectrometry

The repeatability of the E-nose response was assessed using five parallel measurements of GDSR samples and for the GC-MS method was also conducted using two GXSR samples. In the E-nose case, the RSD of the relative peak area and the relative retention time in all common peaks were 1.4% and 1.7%, respectively. The RSD of volatile oil component contents was <1.9% in the GC-MS analysis. This measurement indicated good repeatability of both selected methods.

Data analysis

For qualitative and quantitative data analysis, E-nose response value from 40 s to 80 s of measuring interval was selected as the characteristic value during 120 s data collection. It was assumed that the sensors response values were at a stable condition during the collection time. We performed preprocessing and normalization of the collected data before further pattern recognition. The E-nose data analysis was performed by Bionic Olfactory Odor Analysis Software (BOOAS version 2.0, Guangdong University of Technology, Guangzhou, China).

To acquire the GC-MS data for qualitative and quantitative analysis, the identification of the volatile components was conducted by comparing the recorded mass spectra with the National Institute of Standards and Technology (14.L) mass-spectral library. We compared the outcome with those reported in previous literature and published index data.[22] In addition, the relative content (RC) value of each compound was calculated using the following equations:

$$\bar{X} = \frac{1}{n}\sum_{i=1}^{n} X_i \quad (2)$$

$$S = \sqrt{\frac{1}{n}\sum_{i=1}^{n}(Xi - \bar{X})^2} \quad (3)$$

$$RC = \bar{x} - s \quad (4)$$

Where $\bar{x}$ is mean value; n is equal to 45 (45 = 15 × 3, 15 samples were selected from each group and each sample was analyzed in triplicate); x_i is relative value of each measurement reported from GC–MS, i is from 1 to n; s is the symbol of the SD; RC is the relative content value.

The multivariate data analysis between E-nose data and GC-MS data were performed using the software GenStat (version 18.0th, VSNC). A bioplot of PCA was employed to reveal the effects of those sensors that played a vital role in the classification of the three groups of *AF* samples. A bioplot of PLS was introduced to find the correlations among the three groups of *AF* samples, the E-nose sensors and the volatile oil components contents.

RESULTS AND DISCUSSION

Determination of *Amomi fructus* samples using electronic nose

This section presents the results and discussion of comprehensive aroma characteristics derived from E-nose using radar curves, sensors response, and a bioplot of PCA.

Radar graph

The radar graph in Figure 1 shows that the trend of radar curves has obvious differences among the three groups of *AF* samples. Among all 10 MOS sensors, the S2 was the most sensitive sensor to *AF* aroma.

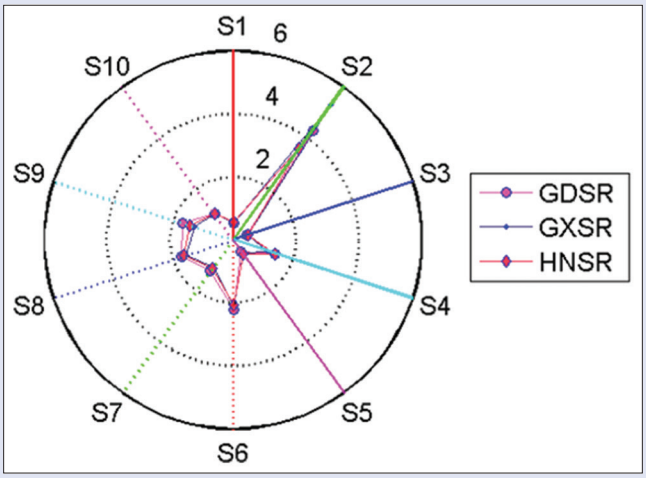

Figure 1: The radar graph of electronic nose for three groups of *Amomi fructus* samples

Moreover, the relative values of S6, S7, S8, and S9 in GDSR samples were more significant than those in GXSR and HNSR samples. While the relative value of the sensor S2 in GXSR samples was bigger than that in GDSR and HNSR samples. The relative value of S4 in HNSR radar curve was the biggest among the three groups of samples. It could be concluded that concentrations of certain fragrant volatile ingredients were different among GDSR, GXSR, and HNSR samples.

Sensor response

Sensor responses of the selected three groups of samples are shown in Figure 2. Overall, the sensor behavior appeared to be similar and each curve consisted of three stages: (1) at the initialization stage, after finishing the cleaning process, the response curve was initialized to value 1 to ensure that all the data collections started at the same level; (2) during the changing stage, the response curve changed rapidly and the maximum slope of curve occurred. The highest rate of change was between 3 s and 40 s. Subsequently, the response curve reached to the stable (stationary) stage; and (3) in the stationary stage, the signals were almost constant and the curve came to a steady state. Meanwhile, the responses of S2 were at the highest values and the responses of S1, S3, and S5 were at the minimum values, as shown in the three plots [Figure 2].

In contrast to those similarities, there were obvious differences among the response curves. For example, S7, S8, and S9 behave differently, especially S9. It reached to the highest level in Figure 2 (GDSR), while GXSR was in the lowest level during the three stages. In addition, some particular sensors such as S1, S4, and S7 had significant changes in the order. It was confirmed that there might be some different volatile compounds among the different growing areas samples, or the concentration of some original compounds in these samples might be different. Therefore, the differences in sensor behaviors of the E-nose guaranteed the rationality of data and provided a reference for qualitative and quantitative analysis for the identification of *AF*.

Bioplot of principal components analysis

To further determine the relationship between sample aroma characteristics and E-nose sensors, a biplot of PCA was conducted. As shown in Figure 3, the first two PCs accounted for 93.90% of the total variance. It was noted that the three different growing areas of *AF* were clearly separated by PCA. Meanwhile, GDSR samples and most of the HNSR samples were located in the region of positive PC1 (61.51%). GXSR samples were distributed in the region of negative PC1. It could lead to the assumption that there was more similarity in the concentrations and categories of aromatic compounds between GDSR and HNSR. Furthermore, as shown in Figure 3, sensors S1, S2, S3, S4, and S5 made a significant contribution in PC2 classification, whereas sensors S6, S7, S8, S9, and S10 weighed more when separating along the PC1 axes. Combined with the sensor characteristics listed in Table 1, it was found that sensors S1, S3, and S5 are sensitive to terpenes and sensors S7, S8, S9, and S10 are sensitive to alcohols and esters. Therefore, it could be assumed that terpenes, alcohols, and esters probably relate more to *AF* identification.

Determination of *Amomi fructus* samples using gas chromatography-mass spectrometry

In this section, the individual aroma components of each group samples were identified by GC-MS. Meanwhile, to study the common and special aroma characteristics among the three groups of *AF*, the contents and species of *AF* were calculated and compared based on GC-MS.

Identification and comparison of volatile compounds among the three groups of Amomi fructus

To find out what characteristic odor components were the key factors that differentiated effectively *AF* from different habitats, volatile compounds were detected by GC-MS and listed in Table 2. As shown in Table 2, there were 65 constituents identified from the three groups of *AF* and these constituents belonged to six chemical classes: terpenes (42), alcohols (12), esters (4), ketones (3), alkanes (2), and aldehydes (2), respectively. Among the 65 compounds, 37 constituents of GDSR comprising 93.51% of the total volatile constituents, 40 constituents of GXSR comprising 97.13% of the total volatile constituents, and 47 constituents of HNSR comprising 97.41% of the total volatile constituents were identified, respectively.

As listed in Table 2, it was noteworthy that terpene components were the most dominant volatiles in *AF* and could be described as typical *AF* flavor constituents, which was consistent with the literature results.[23] By comparison, there were 42 terpene compounds identified in all of the detected *AF* samples; among them, the most abundant component was (1r, 4r)-(+)-campho and its content varied greatly among different habitats, it was 17.588% in GDSR, 23.518% in GXSR and 31.903% in HNSR. Terpinolene also changed much among the three groups, with (0.224%) in GDSR and (0.225%) in HNSR, three times more than that in GXSR (0.064%). (E)-b-farnesene and cubebene were the peculiar terpenes in GDSR. The main special terpene components in GXSR were β-pinene, α-pinene, and 1,6,10-dodecatriene, 7,11-dimethyl-3-methylene-. The main special terpene components in HNSR were (-)-α-copaene, (-)-g-cadinene and

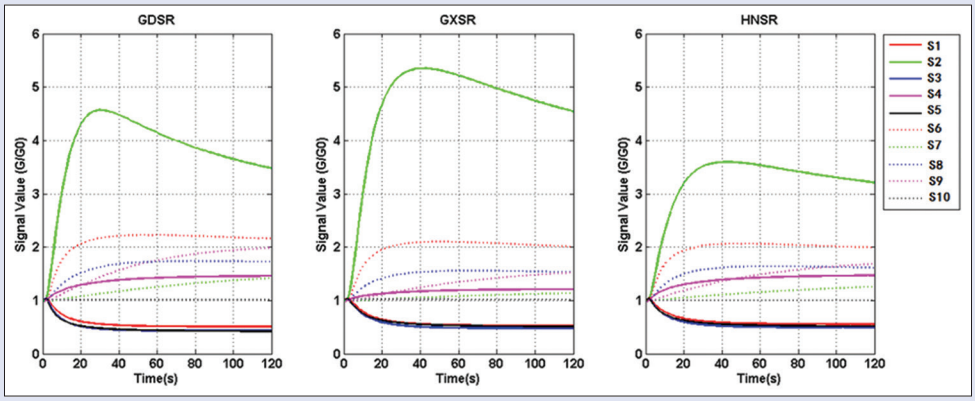

Figure 2: Sensors response of *Amomi fructus* samples from different growing areas. G/G0: the electronic nose sensor response of sample, G0 and G represented the electronic conductivity of sensor when detecting the clean air and sample gas, respectively

Table 2: Volatile compounds of *Amomi fructus* from three different habitats identified by gas chromatography-mass spectrometry

n	RI	Compounds[a]	Formula	Relative content (%), mean±SD			Selected[b]
				GDSR	GXSR	HNSR	
Terpenes							
1	16046	(+)-Dipentene	$C_{10}H_{16}$	6.474±0.542	6.010±1.736	6.485±1.116	
2	16066	Myrcene	$C_{10}H_{16}$	2.660±0.957	2.278±0.663	3.318±1.023	
3	25851	(1r, 4r)-(+)-Campho	$C_{10}H_{16}O$	17.588±2.113	23.518±5.418	31.903±3.781	C1
4	16288	(1s)-(1)-*β*-Pinene	$C_{10}H_{16}$	1.199±0.211	-	4.864±0.687	P1
5	68513	*β*-Caryophyllene	$C_{15}H_{24}$	1.186±0.132	1.111±0.311	6.399±0.890	C2
6	68698	*D*-Cadinene	$C_{15}H_{24}$	0.845±0.041	1.166±0.582	0.882±0.123	C3
7	68576	l-b-Bisabolene	$C_{15}H_{24}$	0.486±0.072	0.570±0.045	1.039±0.114	C4
8	68723	α-Bergamotene	$C_{15}H_{24}$	0.459±0.065	0.248±0.022	-	P2
9	68507	(-)-Germacrene D	$C_{15}H_{24}$	0.450±0.012	1.192±0.314	0.527±0.102	
10	68594	(E)-b-Farnesene	$C_{15}H_{24}$	0.354±0.023	-	-	P3
11	68694	Cyclohexene, 4-(1,5-dimethyl-4-hexenylidene)-1-methyl-, (4Z)-	$C_{15}H_{24}$	0.339±0.009	0.267±0.012	-	P4
12	16095	α-Phellandrene	$C_{10}H_{16}$	0.254±0.013	0.155±0.029	0.158±0.016	C5
13	68580	(-)-Alloaromadendrene	$C_{15}H_{24}$	0.250±0.036	-	0.209±0.091	P5
14	68635	(E)-*α*-Bergamotene, (-)-trans-α-bergamotene	$C_{15}H_{24}$	0.231±0.007	0.425±0.021	-	P6
15	16238	Terpinolene	$C_{10}H_{16}$	0.224±0.074	0.064±0.006	0.225±0.032	C6
16	83535	β-Caryophyllene epoxide	$C_{15}H_{24}O$	0.205±0.042	0.182±0.029	0.699±0.114	C7
17	16078	*γ*-Terpinene	$C_{10}H_{16}$	0.144±0.043	0.095±0.018	0.104±0.061	
18	16251	1,7,7-Trimethyltricyclo[2.2.1.02,6] heptane	$C_{10}H_{16}$	0.096±0.011	0.066±0.008	0.079±0.005	
19	16270	Sabinene	$C_{10}H_{16}$	0.083±0.019	0.063±0.004	-	P7
20	16247	α-Terpinene	$C_{10}H_{16}$	0.074±0.024	-	0.072±0.009	P8
21	68945	Cubebene	$C_{15}H_{24}$	0.019±0.007	-	-	P9
22	16029	Camphene	$C_{10}H_{16}$	5.021±0.486	3.84±1.261	3.729±1.543	C8
23	16224	(1R)-(+)-α-Pinene	$C_{10}H_{16}$	1.748±0.184	-	3.363±0.901	P10
24	68693	(4E)-1-Methyl-4-(6-methylhept-5-en-2-ylidene) cyclohexene	$C_{15}H_{24}$	0.182±0.063	0.146±0.081	0.207±0.041	
25	16269	Bicyclo[3.1.0] hex-2-ene, 4-methyl-1-(1-methylethyl)-	$C_{10}H_{16}$	-	0.076±0.008	0.096±0.017	P11
26	16070	*α*-Pinene	$C_{10}H_{16}$	-	1.012±0.272	-	P12
27	68845	Cyclohexane, 1-ethenyl-1-methyl-2, 4-bis (1-methylethenyl)-, (1S,2S,4R)-	$C_{15}H_{24}$	-	0.680±0.031	0.227±0.014	P13
28	16060	β-Pinene	$C_{10}H_{16}$	-	0.625±0.053	-	P14
29	68665	1,6,10-Dodecatriene, 7,11-dimethyl-3-methylene-	$C_{15}H_{24}$	-	0.446±0.061	-	P15
30	68864	β-selinene	$C_{15}H_{24}$	-	0.346±0.021	-	P16
31	68726	1,5-Cyclodecadiene, 1,5-dimethyl-8-(1-methylethylidene)-, (1E,5E)-	$C_{15}H_{24}$	-	0.213±0.032	-	P17
32	68737	Bicyclo[8.1.0]undeca-2,6-diene, 3,7,11,11-tetramethyl-, (1S,2E,6E,10R)-	$C_{15}H_{24}$	-	1.357±0.203	0.91±0.118	P18
33	68871	Naphthalene, 1,2,4a, 5,8,8a-hexahydro-4,7-dimethyl-1-(1-methylethyl)-, (1S,4aR,8aS)-	$C_{15}H_{24}$	-	0.276±0.053	-	P19
34	68472	(-)-α-Copaene	$C_{15}H_{24}$	-	-	0.937±0.059	P20
35	68698	4,7-dimethyl-1-propan-2-yl-1, 2, 3,5, 6,8a-hexahydronaphthalene	$C_{15}H_{24}$	-	-	0.882±0.115	P21
36	68480	1,4,8-Cycloundecatriene, 2, 6,6, 9-tetramethyl-, (1E,4E,8E)-	$C_{15}H_{24}$	-	-	0.861±0.209	P22
37	68586	1-isopropyl-7-methyl-4-methylene-1, 2, 3,4, 4a, 5, 6, 8a-Octahydronaphthalene	$C_{15}H_{24}$	-	-	0.229±0.052	P23
38	68910	(-)-g-Cadinene	$C_{15}H_{24}$	-	-	0.226±0.076	P24
39	68696	((-)-1-[(1R)-1,5-Dimethyl-4-hexenyl]-4-methyl-1,4-cyclohexadiene	$C_{15}H_{24}$	-	-	0.124±0.051	P25
40	68788	(-)-Isocaryophyllene	$C_{15}H_{24}$	-	-	0.12±0.045	P26
41	24654	(3E)-4,8-dimethylnona-1,3,7-triene	$C_{11}H_{18}$	-	-	0.105±0.008	P27
42	68510	Naphthalene, 1,2,3,4,6,7,8,8a-octahydro-1,8a-dimethyl-7-(1-methylethenyl)-, (1R,7R,8aS)-	$C_{15}H_{24}$	-	-	0.077±0.013	P28
Alcohols							
43	27447	Linalool	$C_{10}H_{18}O$	0.408±0.064	0.570±0.092	0.7±0.042	C9
44	27498	Terpinen-4-ol	$C_{10}H_{18}O$	0.352±0.041	0.274±0.061	0.403±0.068	
45	83704	Espatulenol	$C_{15}H_{24}O$	0.295±0.042	-	0.51±0.032	P29
46	27485	Borneol	$C_{10}H_{18}O$	0.118±0.018	0.034±0.006	0.106±0.018	C10
47	83508	(Z)-α-Santalol	$C_{15}H_{24}O$	0.110±0.042	-	-	P30
48	27458	Cineole	$C_{10}H_{18}O$	0.102±0.006	0.116±0.021	0.356±0.093	C11
49	85751	Nerolidol	$C_{15}H_{26}O$	-	1.280±0.256	-	P31
50	85758	trans-Nerolidol	$C_{15}H_{26}O$	-	0.703±0.083	-	P32
51	85748	Farnesol	$C_{15}H_{26}O$	-	2.521±0.438	-	P33
52	27823	L(-)-Borneol	$C_{10}H_{18}O$	-	1.317±0.152	0.342±0.021	P34
53	85684	cis-Nerolidol	$C_{15}H_{24}$	-	-	0.719±0.046	P35
54	85776	β-Bisabolol	$C_{15}H_{26}O$	-	-	0.726±0.103	P36

Contd...

Table 2: Contd...

n	RI	Compounds[a]	Formula	Relative content (%), mean±SD			Selected[b]
				GDSR	GXSR	HNSR	
Esters							
55	61655	Bornyl acetate	$C_{12}H_{20}O_2$	50.793±6.492	40.543±8.112	23.169±4.802	C12
56	47804	Methyl 6, 6-dimethylbicyclo[3.1.1] hept-3-ene-4-carboxylate	$C_{11}H_{16}O_2$	0.085±0.016	-	0.474±0.064	P37
57	124930	(2E,6E)-Farnesyl acetate	$C_{17}H_{28}O_2$	-	3.888±0.645	-	P38
58	59493	(1s)-6,6-dimethylbicyclo (3.1.1) hept-2-ene-2-methanol acetate	$C_{12}H_{18}O_2$	-	-	0.035±0.004	P39
Ketones							
59	24605	(-)-Myrtenal	$C_{10}H_{14}O$	0.208±0.048	0.219±0.053	0.826±0.105	C13
60	24351	Bicyclo[3.1.1]heptan-3-one, 6,6-dimethyl-2-methylene-	$C_{10}H_{14}O$	0.080±0.006	-	0.171±0.062	P40
61	121299	(3E)-4-[(1S,4aS,8aS)-5,5,8a-Trimethyl-2-methylenedecahydro-1-naph thalenyl]-3-buten-2-one	$C_{18}H_{28}O$	-	-	0.137±0.024	P41
Alkanes							
62	15146	1-Isopropyl-2-methylbenzene	$C_{10}H_{14}$	0.115±0.021	0.230±0.017	-	P42
63	15143	1-Isopropyl-4-methylbenzene	$C_{10}H_{14}$	0.115±0.006	-	0.399±0.026	P43
Aldehydes							
64	96781	Bicyclohomofarnesal	$C_{16}H_{26}O$	0.160±0.022	0.163±0.038	0.144±0.027	
65	81719	(E)-5-(2,3-dimethyltricyclo[2.2.1.02,6] hept-3-yl)-2-methylpent-2	$C_{15}H_{22}O$	-	-	0.158±0.114	P44

[a]Compounds identified via GC-MS analysis based on comparison with the RI and the mass spectra of standard compounds (similarity adinene) ene))-g-Cad[b]Selected: 13 common compounds and 44 specific compounds were selected according to the two criteria described in Section *PCA based on GC-MS data*. NIST: National Institute of Standards and Technology; "-": Not detected; SD: Standard Deviation; GDSR: Guangdong Sharen; GXSR: Guangxi Sharen; HNSR: Hainan Sharen; RI: Retention Indices

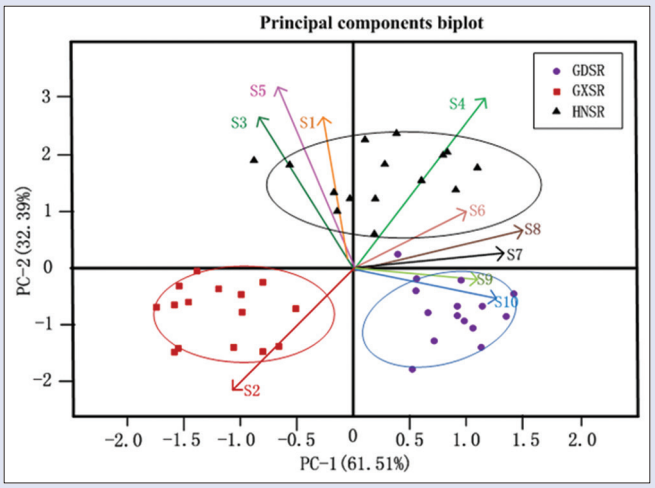

Figure 3: Bioplot of principal component analysis based on the electronic nose data

4,7-dimethyl-1-propan-2-yl-1,2,3,5,6, 8a-hexahydronaphthalene, etc., It could be concluded that there were much difference between the terpene species and contents among the three groups of AF, which can be used as a basis for distinguishing aroma of AF from different habitats.

For alcohols, the RC of GXSR (6.815%) was much higher than that of HNSR (3.862%) and GDSR (1.385%). Four compounds were identified as common compositions: linalool, terpinen-4-ol, borneol, and cineole. Espatulenol was detected in GDSR and HNSR; L(-)-borneol was identified in GXSR and HNSR. For special alcohol compounds, (Z)-α-santalol was identified in GDSR; nerolidol, trans-nerolidol and farnesol were determined in GXSR; β-bisabolol and cis-nerolidol were identified in HNSR.

The content of esters was the highest among the six chemical classes listed in Table 2. The only common esters compound identified from the three groups of samples was bornyl acetate. It is the main active ingredient and has been considered as the quality control component in AF, which has been reported in Chinese Pharmacopoeia 2015 Edition.[2] In the three groups of samples, bornyl acetate was detected 50.793% in GDSR, 40.543% in GXSR, and 23.169% in HNSR, respectively. Thus, it has been said that AF cultivated in Guangdong Province has the best quality.[1] In addition, methyl 6,6-dimethylbicyclo[3.1.1]hept-3-ene-4-carboxylate was identified in GDSR and in HNSR; (2E, 6E)-farnesyl acetate was detected in GXSR; and (1s)-6, 6-dimethylbicyclo (3.1.1) hept-2-ene-2-methanol acetate was detected in HNSR.

The (-)-myrtenal was the only common ketones compound identified in all the samples. The RC was 0.208% in GDSR, 0.219% in GXSR, and 0.826% in HNSR, respectively. For individual compounds, (3E)-4-[(1S, 4aS, 8aS)-5, 5, 8a-Trimethyl-2-methylenedecahydro-1-naph thalenyl]-3-buten-2-one was identified in HNSR. Maybe, ketones compounds were also effective in distinguishing AF from different habitats.

The contents of alkanes and aldehydes were relatively lower than the other classes in *AF*. For aldehydes, bicyclohomofarnesal was identified in all samples, GDSR (0.16%), GXSR (0.163%), and HNSR (0.244%). It seemed that alkanes and aldehydes might play a minor contribution in discriminating among AF species.

From the above analysis, it has been shown that those common compounds identified in all *AF* samples are presenting their similarity in both aroma characteristics and the treatment for digestive diseases. However, obvious variations in concentrations of common ingredients and different species in specific components might illustrate their differences and provide possible markers for their identification. This might further clarify different responses of E-nose sensors. Therefore, different aroma constituents with different concentrations had caused different sensor responses, revealing a potential relationship between individual aroma compounds and fragrance fingerprint.

Principal components analysis based on gas chromatography-mass spectrometry data

To determine which volatile components play important role in distinguishing *AF* from different habitats, 57 possible aroma constituents including 13 common compounds and 44 specific compounds were selected. The selection criteria were: (1) for common

compounds among the three groups, those compounds with obvious difference in contents were chosen and (2) All specific components that were considered important to differentiating the three groups of *AF* were chosen. Hence, a total of 57 constituents including 35 terpenes, 12 alcohols, 4 esters, 3 ketones, 2 alkanes, and 1 aldehyde were chosen. Figure 4 shows the bioplot of PCA based on the 13 common components and Figure 5 shows the bioplot of PCA based on 44 special compounds.

It can be observed that three groups of *AF* samples of different habitats were distributed in different regions in Figures 4 and 5. The PCA plot of samples and the contribution rates of PC1 and PC2 were 61.35% and 34.65%, respectively [Figure 4]. The total contribution rate of the first two PCs was 96%. The contribution rates of PC1 and PC2 were 59.13% and 31.07%, respectively [Figure 5]. The total contribution rate of PC1 and PC2 was 90.2%. Both of which performed similar to the E-nose data. Thus, the results of GC-MS analysis were consistent with the results of E-nose analysis.

In Figure 4, samples of GDSR and HNSR fell in the upper quadrants of PC2, while samples of GXSR fell in the lower quadrants of PC2, which showed that GDSR and HNSR demonstrated more similarities in the components of d-cadinene, (-)-germacrene D, terpinolene, and borneol. However, HNSR located in the right of PC1, GDSR and GXSR located in the left of PC1, which presented GDSR and GXSR had more similarities in (1r, 4r)-(+)-campho, cineole, (-)-myrtenal, l-b-Bisabolene,β-Caryophyllene epoxide, and bornyl acetate.

Figure 5 shows most of the special compounds that discriminate *AF* of different habitats. The α-bergamotene, (E)-b-farnesene, sabinene, cubebene, and (Z)-α-santalol located near the negative axis of PC2, which revealed that these components played much important role in distinguishing the GDSR samples from the other two samples. Similarly, the (-)-α-copaene and cis-nerolidol located near the positive axis of PC1indicate that these compounds contributed more in distinguishing the HNSR samples from others. Furthermore, α-pinene, β-pinene, nerolidol, trans-nerolidol, and farnesol played vital role in distinguishing GXSR from the other two samples. The above-mentioned components were mainly terpenes, alcohols, esters, and ketones, which were highly consistent with the previous analysis (Section *Identification and comparison of volatile compounds among the three groups of AF*). Hence, the next step was to investigate the internal relationship between effective volatile constituents and E-nose sensors.

Correlation analysis between electronic nose and gas chromatography-mass spectrometry

To investigate the correlation between response characteristics of E-nose and volatile compounds by GC-MS, the PLS was performed on the 57 selected volatile constituents and 10 sensors and their correlation is shown in the bioplot of [Figure 6].

It can be observed that the response of sensors S1, S3, S5, S7, S8, and S9 were all distributed in the right quadrants of Factor 1 in the coordinate system [Figure 6]. Moreover, they surrounded by terpenes, alcohols, and esters, such as (1r, 4r)-(+)-campho, (1s)-(1)-β-pinene, β-caryophyllene, d-cadinene, camphene, (1r)-(+)-α-pinene, borneol, and bornyl acetate. The shorter the distance between samples in the bioplot, indicates the higher the correlation the selected six sensors (sensors S1, S3, S5, S7, S8, and S9) and nearby volatile constituents. Hence, it revealed that the six sensors: S1, S3, S5, S7, S8, and S9, were greatly associated with those terpenes, alcohols, and esters. This result was highly agreed with those previous reported results in section bioplot of PCA [Figure 3] and section PCA based on GC-MS data [Figures 4 and 5]. Therefore, it might be concluded that some of these terpenes, alcohols, and esters interacted with the six sensors. During the E-nose detection, these interactions had caused different sensors behaviors and resulted in successful classification of *AF*. Thus, it could be assumed that the concentrations of those chemical constituents contributing most in discriminating three groups of *AF* and could be used to predict the growing region of AF by the highly related sensors.

Chemical constituents prediction by electronic nose sensors in partial least squares

On the basis of correlation analysis between selected E-nose sensors and crucial volatile compounds, 6 MOS sensors (S1, S3, S5, S7, S8, and S9) and 12 volatile constituents ((1r, 4r)-(+)-campho, β-caryophyllene, D-cadinene, camphene, borneol, and bornyl acetate (from the shared compounds); (E)-b-farnesene, cubebene (from

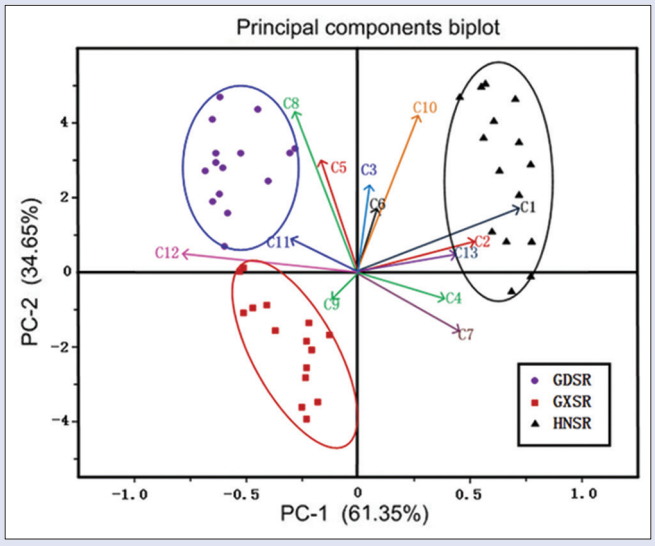

Figure 4: Bioplot of principal components analysis based on 13 shared aroma constituents

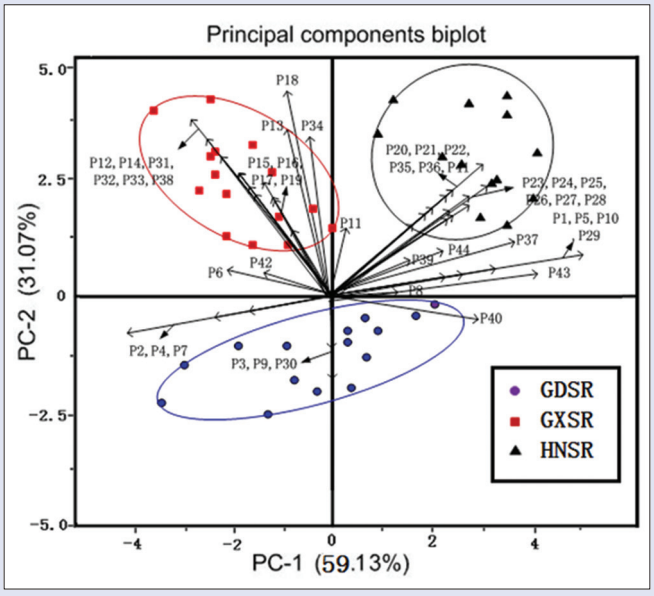

Figure 5: Bioplot of principal components analysis based on 44 special aroma constituents

Table 3: Regression coefficients between the relative content of 12 volatile constituents and response values of six sensors

B	a											
	C1	C2	C3	C8	C10	C12	P3	P9	P12	P16	P20	P24
$constant	19.5062	0.8421	0.7916	3.7424	0.0954	21.3153	0.0749	0.0237	0.9755	0.2167	0.7524	0.1879
S1	0.4981	0.0747	0.0729	0.1138	0.0603	2.0901	0.0567	0.0017	0.0146	0.0187	0.0436	0.0014
S3	1.1512	0.1119	0.0745	0.0932	0.0543	1.6749	0.0598	0.0091	0.0044	0.0564	0.0125	0.0095
S5	0.6531	0.0827	0.0661	0.052	0.0505	1.0759	0.1546	0.0074	0.4402	0.1546	0.0432	0.0088
S7	0.5932	0.8517	0.0836	0.3535	0.0983	0.1825	0.0434	0.0109	0.0229	0.0143	0.0109	0.0229
S8	1.1546	0.6033	0.1076	0.0537	0.0767	0.1479	0.0712	0.0088	0.9754	0.0712	0.0888	0.0054
S9	0.5614	0.0983	0.871	0.2218	0.1156	0.0654	0.0422	0.0221	0.0476	0.0322	0.1221	0.0876

[a]The 12 volatile constituent; [b]The six sensors; C1: (1r, 4r)-(+)-Campho; C2: β-Caryophyllene; C3: D-Cadinene; C8: Camphene; C10: Borneol; C12: Bornyl acetate; P3: (E)-b-farnesene; P9: Cubebene; P12: α-Pinene; P16: β-Selinene; P20: (-)-α-Copaene; P24: (-)-g-Cadinene

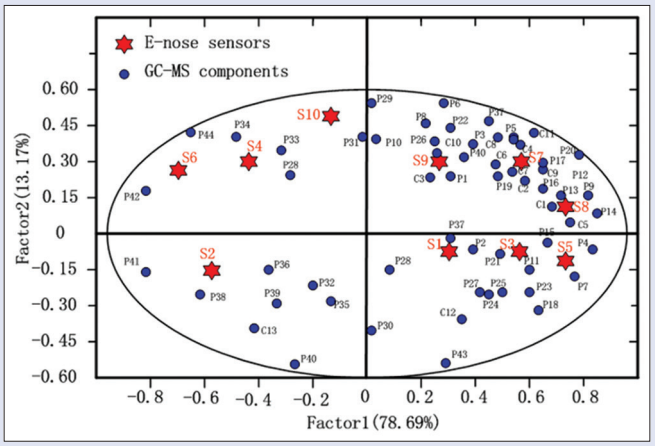

Figure 6: Bioplot for correlation between volatile constituents and electronic nose sensors

Table 4: Prediction of partial least squares model

Volatile constituents	$(Rc)^2$	RMSEC	$(Rp)^2$	RMSEP
(1r, 4r)-(+)-Campho	0.931	0.674	0.902	0.721
β-Caryophyllene	0.863	1.083	0.811	1.194
D-Cadinene	0.902	0.549	0.897	0.771
Camphene	0.947	0.531	0.879	0.828
Borneol	0.954	0.418	0.93	0.493
Bornyl acetate	0.925	0.616	0.911	0.643
(E)-b-Farnesene	0.927	0.662	0.909	0.833
Cubebene	0.956	0.417	0.931	0.463
α-Pinene	0.937	0.602	0.919	0.686
β-Selinene	0.944	0.661	0.904	0.811
(-)-α-Copaene	0.872	0.955	0.849	1.045
(-)-g-Cadinene	0.931	0.739	0.865	0.894

$(Rc)^2$: Determination coefficient of calibration; $(Rp)^2$: Determination coefficient of prediction; RMSEC: Root mean square of calibration; RMSEP: Root mean square error of prediction

GDSR); α-pinene, β-selinene (from GXSR); and (-)-α-copaene and (-)-g-cadinene (from HNSR) were selected for qualitative analysis using PLS. Six sensors were used as independent variables and the RC s of 12 volatile constituents were used as dependent variables. 45 samples (15 GDSR data, 15 GXSR data and 15 HNSR data) were used for PLS training and 15 samples (5 GDSR data, 5 GXSR data, and 5 HNSR data) were used for PLS testing. After finishing the training, the PLS correlation models between the six MOS sensors and the RC s of the 12 volatile constituents were calculated [Table 3]. Moreover, the determination coefficient of calibration ($(R_c)^2$) was used to evaluate the PLS model and the determination coefficient of prediction ($(R_p)^2$) was employed to evaluate the prediction. At the same time, the root mean square of calibration (RMSEC) and the root mean square error of prediction (RMSEP) values were calculated. The results are shown in Table 4 and Figure 7.

The selected 12 compounds could be accurately evaluated with $(R_c)^2$ and $(R_p)^2$ [Figure 7] and most of the values of $(R_c)^2$ and $(R_p)^2$ were >0.90, excepting β-caryophyllene (0.863 for $(R_c)^2$ and 0.811 for $(R_p)^2$) and (-)-α-copaene (0.872 for $(R_c)^2$ and 0.849 for $(R_p)^2$). These results were confirmed by the RMSEC and RMSEP values in Table 4. It can be concluded that the quantitative characteristics of volatile chemical constituents can be predicted and explained by E-nose data analysis.

CONCLUSION

In this work, the aroma characteristics of *AF* from three representative growing areas were investigated and analyzed using comprehensive odor and individual fragrance components by employing E-nose and GC-MS. The E-nose performed well in identifying *AF* from the three different habitats with its COM sensors and PCA data analysis achieving 93.90% of the variance. Moreover, during chemical component analysis, it was demonstrated that the differences among the three groups of *AF* aroma were possibly caused by 65 aroma constituents of three *AF* groups which were identified by GC-MS. Comparing the detailed profiles of each component, terpenes, alcohols, and esters were the main components used to distinguish *AF*. Especially, the contents of (1r, 4r)-(+)-campho and bornyl acetate accounted for >55% of the total volatile constituents (68.4% in GDSR, 64.0% in GXSR, and 55.1% in HNSR), which were the key indexes to identify the quality of *AF*. After comparing and analyzing the interrelation between aroma constituents and E-nose sensors, it was indicated that the six sensors (S1, S3, S5, S7, S8, and S9 in PEN3) were highly related to most aroma compounds of *AF*. Therefore, three main volatile components: terpenes, alcohols, and esters, might have caused the changing behavior of the sensors. Furthermore, the response of these sensors varied with the concentration of volatile compounds, which enabled the E-nose to differentiate the three groups of *AF* successfully. To confirm the correlation of the contents of 12 aroma ingredients and the response values of six E-nose sensors, we employed a trained PLS (45 samples for training and 15 samples for testing). Finally, a satisfied quantitative prediction was presented with $(R_c)^2$ and $(R_p)^2$ of about 90%. It appears that the E-nose can provide an easy-operating, accurate, and nondestructive approach for determining *AF* species and predict the contents of critical aroma components, offering a promising reference for the future studies on intelligent monitoring and quality control of herbal medicine.

Financial support and sponsorship

The authors acknowledge the financial support of the General Program of the National Natural Science Fund (Grant No. 61571140), Guangdong Provincial Project (Grant No. 2016A020226018), Guangdong Provincial Administration of traditional Chinese Medicine Project (Grant No. 20161152), Guangdong University Project (Grant No. 51348000).

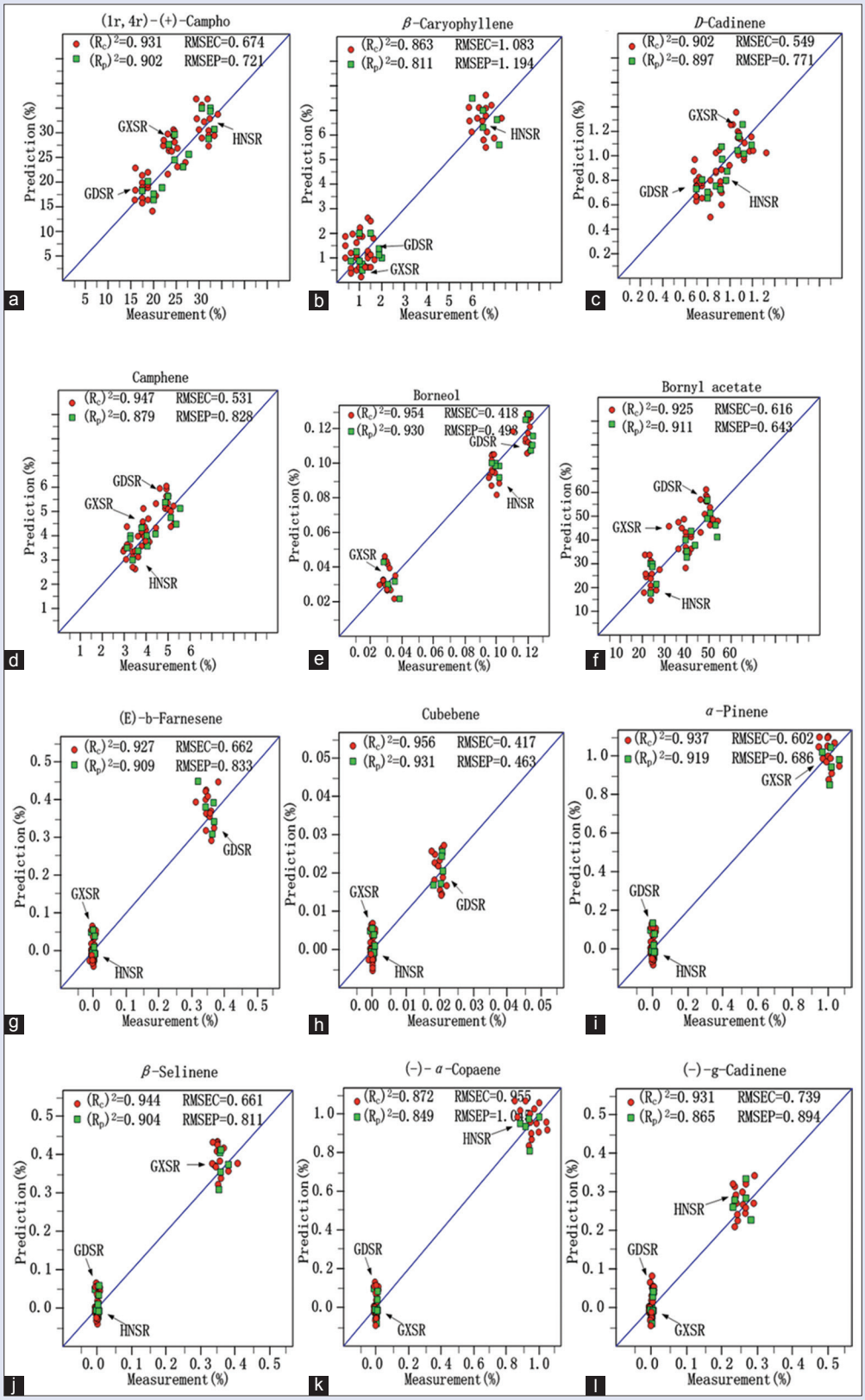

Figure 7: The scatter plot of measured contents and predicted contents of the 12 selected constituents: (a) 1r, 4r)-(+)-Campho; (b) β-Caryophyllene; (c) D-Cadinene; (d) Camphene; (e) Borneol; (f) Bornyl acetate; (g) (E)-b-Farnesene; (h) Cubebene; (i) α-Pinene; (j) β-selinene; (k) (-)-α-Copaene; (l) (-)-g-Cadinene)

Conflicts of interest

There are no conflicts of interest.

REFERENCES

1. Li G, Li XL, Tang DY, Li HT, Wang YQ, Li YH. Quality of commercial *Amomum villosum*. Zhongguo Zhong Yao Za Zhi 2016;41:1608-16.
2. National Pharmacopoeia Committee. Pharmacopoeia of the People's Republic of China, Part I. Beijing, China: China Medical Science Press; 2015. p. 385.
3. Huang CC. The research progress on chemical constituents, pharmacological action and clinical application of *Amomi fructus*. J Tradit Chin Med 2017;11:210-2.
4. Zhang T, Lu SH, Bi Q, Liang L, Wang YF, Yang XX, *et al*. Volatile oil from *Amomi fructus* attenuates 5-fluorouracil-induced intestinal mucositis. Front Pharmacol 2017;8:786.
5. Yan Y, Jin ML, Zhou L, Liu HF, Chen CM, Xin Y. Regulatory effect of herbal medicine fructus amomi on antibiotic-induced intestinal flora imbalance in mice. Chin J Microecol 2013;25:1040-3.
6. Quan Q, Lin JC, Liang JM, Zhang LH, Jiang XH. Compare on the content of bronyl acetate and total volatile oil in fructus amomi from different producing area. Guiding J Tradit Chin Med Pharm 2017;23:70-2.
7. Zou HQ, Gong JT, Zhao LY, Tao O, Li JH, Ren ZH, *et al*. Quality and quantity classification models of fructus amomi applying electronic nose with multiple mathematical statistics methods. J Int Pharm Res 2015;42:513-8.
8. Li ML, Dai GB, Chang TY, Shi CC. Accurate determination of geographical origin of tea based on terahertz spectroscopy. Appl Sci 2017;7:172.
9. An XQ, Li ZZ, She LG. Chemical constituents of *Amomi fructus* lour. Nat Prod Res Dev 2011;23:1021-4.
10. Li SM, Qiang YE, Hui AO. Relationship between the GC-MS fingerprints of essential oil from fructus amomi and its analgesia effect. Chin Tradit Pate Med 2016;38:346-50.
11. Loutfi A, Coradeschi S, Mani GK, Shankar P, Rayappan JB. Electronic noses for food quality: A review. J Food Eng 2015;144:103-11.
12. Jiang S, Wang J, Wang YW, Cheng SM. A novel framework for analyzing MOS E-nose data based on voting theory: Application to evaluate the internal quality of Chinese pecans. Sens Actuators B Chem 2017;242:511-21.
13. Fitzgerald JE, Bui ET, Simon NM, Fenniri H. Artificial nose technology: Status and prospects in diagnostics. Trends Biotechnol 2017;35:33-42.
14. Zhu L, Li B, Liu X, Huang G, Meng X. Isolation and purification of schisandrol A from the stems of *Schisandra chinensis* and cytotoxicity against human hepatocarcinoma cell lines. Pharmacogn Mag 2015;11:131-5.
15. Majchrzak T, Wojnowski W, Dymerski T, Gębicki J, Namieśnik J. Electronic noses in classification and quality control of edible oils: A review. Food Chem 2018;246:192-201.
16. Gancarz M, Wawrzyniak J, Gawrysiak-Witulska M, Wiacek D, Nawrocka A, Tadla M, *et al*. Application of electronic nose with MOS sensors to prediction of rapeseed quality. Measurement 2017;103:227-34.
17. Fan H, Bennetts VH, Schaffernicht E, Lilienthal AJ. A cluster analysis approach based on exploiting density peaks for gas discrimination with electronic noses in open environments. Sens Actuators B Chem 2018;259:183-203.
18. Villarreal CC, Pham T, Ramnani P, Mulchandani A. Carbon allotropes as sensors for environmental monitoring. Curr Opin Electrochem 2017;3:106-13.
19. Chen Q, Song J, Bi J, Meng X, Wu X. Characterization of volatile profile from ten different varieties of Chinese jujubes by HS-SPME/GC-MS coupled with E-nose. Food Res Int 2018;105:605-15.
20. Zhou X, Wan J, Chu L, Liu W, Jing Y, Wu C. Identification of sulfur fumed Pinelliae Rhizoma using an electronic nose. Pharmacogn Mag 2014;10:S135-40.
21. Li D, Lei T, Zhang S, Shao XY, Xie CS. A novel headspace integrated E-nose and its application in discrimination of Chinese medical herbs. Sens Actuators B Chem 2015;221:556-63.
22. Liu MC, Zou XH, Lan LL, Cao C, Jiang B, Zeng YE. Discrimination of A*romi fructus* from different origins using electronic nose combined with headspace-gas chromatography-mass spectrometry coupled and chemometrics. Chin J Experi Tradit Med Formulae 2017;23:35-42.
23. Ye Q, Li SM, Ao H, Chen L, Li H ×. Comparison of the compositions in volatile oil from *Amomum villosum* from different habitats. Chin Tradit Patent Med 2014;36:1033-7.